Journal of Sound and Vibration (1997) **205**(1), 33–55

EFFECT OF PARTIAL DEPTH CRACKS ON THE NATURAL FREQUENCY OF TWISTED BLADES: A 3-D FINITE ELEMENT ANALYSIS

S. Neogy and V. Ramamurti

Department of Applied Mechanics, Indian Institute of Technology, Madras—600 036, *India*

(*Received* 14 *May* 1996, *and in final form* 11 *February* 1997)

It is possible that fatigue cracks may appear in turbomachine blades which are subjected to extreme conditions during operation. Such cracks may become the cause of failure. The feasibility of considering the natural frequency as a parameter for detecting full depth cracks has been considered earlier. The present paper not only compares the result for full depth cracks with the previous work but also presents results for partial depth cracks. It concludes with the suggestion that the natural frequency is too poor a parameter for the diagnosis of partial depth cracks. However, experimental verification is suggested and a cautionary note about extrapolation of conclusions to rotating structures is also provided.

1. INTRODUCTION

The conventional subject of fracture mechanics presupposes the presence of a crack and, based upon this, it calculates necessary parameters such as the stress intensity factor, the strain energy release rate, etc., in order that they may be compared with the corresponding critical values and a decision taken as to whether the crack is propagating. Here lies the contribution of fracture mechanics in providing better designs and estimation of their life. However, at the same time it need be stressed that knowledge of the crack size and geometry has to be obtained from previous experience, or from a database, for the whole process to work.

Turbomachinery has for a long time been a technical field of practical importance. The blade of a turbomachine is a critical component because it possesses a complicated structural geometry (taper, stagger and non-uniform twist), a loading cycle due to fluid pressure which is rather difficult to specify accurately, centrifugal effects due to rotation at high speed and boundary conditions that are not that simple. All of these factors go to make the vibrational behaviour of a rotating blade an important, serious and difficult problem.

Subjected to such extreme conditions as mentioned above, a turbine blade is prone to develop fatigue cracks which might not exist in a form detectable by standard NDT techniques before its actual operation. As such, engineers of today are placing emphasis upon diagnosing the presence of cracks. The investigations concerning the vibrational behaviour of a cracked blade are to determine whether and in what manner a crack may be recognized by measuring the blade vibration, in order that large consequent damage is prevented.

The possibility of the natural frequency being considered as a criterion for damage detection has been considered in reference [1], where the effect of a full depth crack on

0022–460X/97/310033 + 23 $25.00/0/sv970991

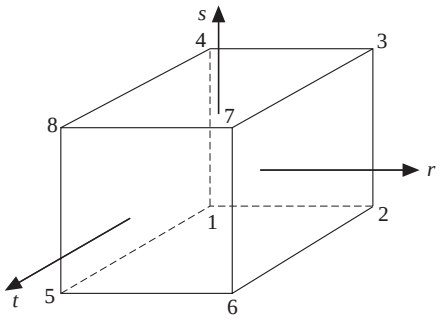

Figure 1. The 3-D brick element.

the natural frequency of a pretwisted blade has been studied. However, in practice, during inception, a crack will only have a depth that is a fraction of the thickness of the blade. The objective of the present work is not only to determine the natural frequency of blades (assumed to be non-rotating) possessing partial depth cracks which may be considered non-propagating, but also to analyze full depth cracks and compare the results with those of reference [1].

TABLE 1

Frequency parameters $\sqrt{\rho t \omega^2 a^4/D}$ *for an uncracked square cantilevered plate of thickness ratio* 20 *in various modes and for various values of pretwist*

Pretwist	Mesh type	Mode 1	Mode 2	Mode 3	Mode 4	Mode 5
0	10 × 10 × 1	3·452	8·330	20·741	25·965	29·758
	20 × 20 × 4	3·474	8·373	21·023	26·504	30·133
	Figure 2	3·485	8·405	20·949	26·330	30·108
	Reference [26]	3·451	8·327	20·730	25·950	29·750
15	10 × 10 × 1	3·426	10·268	20·084	25·847	30·796
	20 × 20 × 4	3·448	10·322	20·313	26·458	31·200
	Figure 2	3·459	10·346	20·264	26·217	31·147
	Reference [26]	3·429	10·260	20·080	25·840	30·790
30	10 × 10 × 1	3·353	14·233	18·278	25·919	33·396
	20 × 20 × 4	3.373	14.313	18.412	26.556	33.878
	Figure 2	3·384	14·321	18·403	26·299	33·751
	Reference [26]	3·351	14·230	18·270	25·910	33·360
45	10 × 10 × 1	3.246	15.984	18.261	26.311	36.506
	20 × 20 × 4	3·262	16·042	18·374	26·962	37·091
	Figure 2	3·272	16·060	18·364	26·692	36·865
	Reference [26]	3·243	15·970	18·250	26·290	36·470
60	10 × 10 × 1	3·119	13·762	21·619	26·755	39·272
	20 × 20 × 4	3·128	13·764	21·762	27·400	39·949
	Figure 2	3·138	13·797	21·730	27·119	39·621
	Reference [26]	3·115	13·740	21·620	26·710	39·200

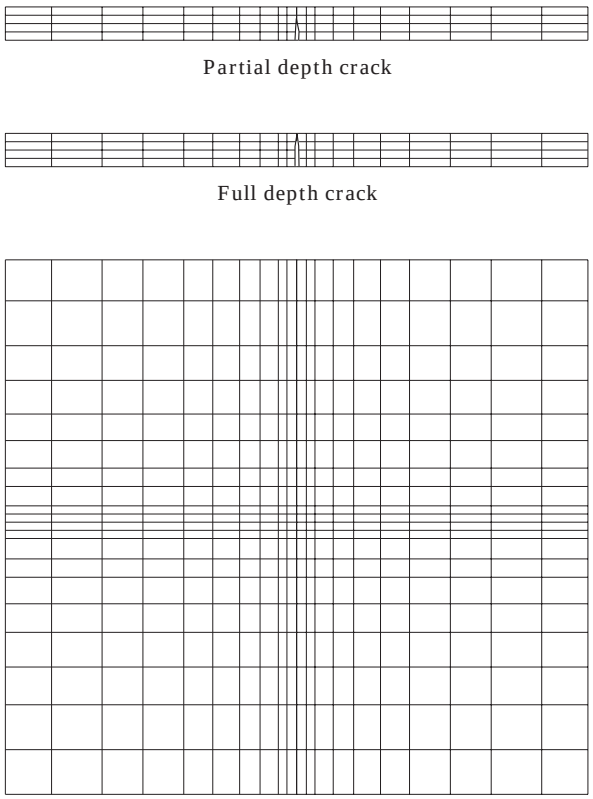

Figure 2. The non-uniform mesh for an untwisted square cantilevered blade (blade thickness and crack width exaggerated for clarity).

TABLE 2

The core and labour required to solve a full depth crack of type I (relative crack length = 0·5) by using a triangular plate and a brick element

	Core					Labour
Element type	No. of nodes	No. of elements	No. of eqns	Max. band width	Profile	Time
Plate	451	800	2580	~ 192	0·313122E6	R 3 m 28·45 s U 0 m 25·41 s S 0 m 0·03 s
Brick	2255	1600	6450	~ 3471	1·833780E6	R 1 h 9 m 30·91 s U 8 m 28·85 s S 0 m 0·03 s

Note that these values are not the maximum possible required to solve a crack problem. For a different crack configuration, they may be higher. They only represent the trend and are given so as to compare the two elements.

R, U and S represent real time (clock time), user time and system time, respectively, on an IBM RS 6000 mainframe system.

2. ANALYSIS

2.1. CRACK MODELS: A REVIEW

Cracks in structures and machines produce local changes in the flexibility of the structure and thereby alter its dynamic characteristics. Such problems have been studied by several researchers, and reviews and literature surveys have also been reported in references [2–4].

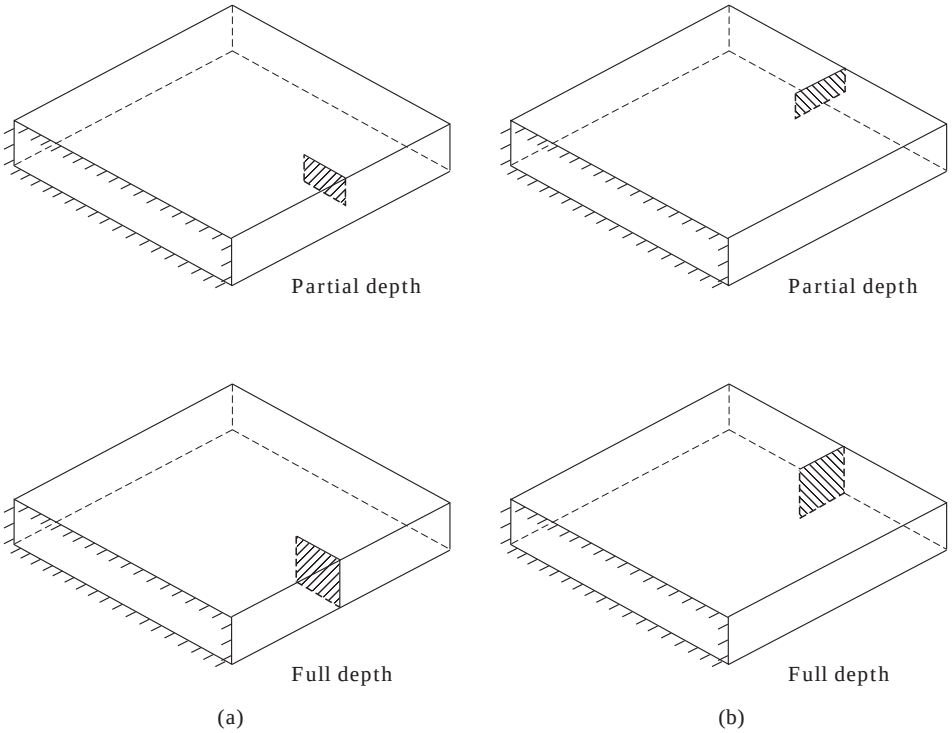

Figure 3. Various configurations of the square cracked cantilevered blade (untwisted case only shown) with a full and a partial depth crack. (a) Crack type I; (b) crack type II.

TABLE 3

Frequency parameters $\sqrt{\rho t\omega^2 a^4/D}$ *for a square cantilevered untwisted plate for various crack types* (*full depth*) *and lengths in different modes*

Crack type	c/a	Mode 1	Mode 2	Mode 3	Mode 4	Mode 5
I and full depth	0·1	3·483	8·425	20·909	26·741	30·313
	0·2	3·443	8·109	19·989	26·035	29·446
	0·3	3·367	7·549	18·703	24·694	28·885
	0·4	3·245	6·809	17·333	22·925	28·682
	0·5	3·058	6·040	16·005	21·314	28·313
II and full depth	0·1	3·506	8·473	21·556	26·119	30·726
	0·2	3·507	8·229	21·189	24·506	28·438
	0·3	3·507	7·731	20·397	22·983	24·737
	0·4	3·498	6·955	18·924	21·056	22·044
	0·5	3·497	6·037	17·406	18·797	21·698

TABLE 4

Frequency parameters $\sqrt{\rho t\omega^2 a^4/D}$ *for a square cantilevered plate (pretwist* $= 15$ *and thickness ratio* $= 50$*) for various crack types (full depth) and lengths in different modes*

Crack type	c/a	Mode 1	Mode 2	Mode 3	Mode 4	Mode 5
I and full depth	0·1	3·460	16·395	20·418	28·362	37·718
	0·2	3·424	13·997	19·650	27·537	36·686
	0·3	3·359	11·308	18·581	26·460	35·468
	0·4	3·256	8·952	17·370	25·058	34·352
	0·5	3·096	7·161	16·108	23·719	31·823
II and full depth	0·1	3·482	16·664	21·107	28·092	36·794
	0·2	3·483	14·569	20·967	26·514	33·011
	0·3	3·483	11·852	20·867	24·525	28·540
	0·4	3·474	9·246	20·522	22·565	24·435
	0·5	3·473	7·181	20·037	21·189	21·609

TABLE 5

Frequency parameters $\sqrt{\rho t\omega^2 a^4/D}$ *for a square cantilevered plate (pretwist* $= 30$ *and thickness ratio* $= 50$*) for various crack types (full depth) and lengths in different modes*

Crack type	c/a	Mode 1	Mode 2	Mode 3	Mode 4	Mode 5
I and full depth	0·1	3·391	18·710	27·048	32·728	50·601
	0·2	3·361	18·107	21·020	32·156	49·487
	0·3	3·310	15·265	17·338	31·268	46·342
	0·4	3·230	11·169	16·354	29·599	41·473
	0·5	3·106	8·383	15·279	27·361	37·610
II and full depth	0·1	3·413	19·306	27·470	33·093	47·178
	0·2	3·413	19·211	21·845	31·921	40·715
	0·3	3·413	15·619	19·179	30·288	35·223
	0·4	3·402	11·061	18·944	28·446	30·593
	0·5	3·401	8·907	18·866	26·694	27·019

TABLE 6

Frequency parameters $\sqrt{\rho t\omega^2 a^4/D}$ *for a square cantilevered plate (pretwist* $= 45$ *and thickness ratio* $= 50$*) for various crack types (full depth) and lengths in different modes*

Crack type	c/a	Mode 1	Mode 2	Mode 3	Mode 4	Mode 5
I and full depth	0·1	3·287	16·404	34·313	38·266	52·371
	0·2	3·262	15·968	24·864	38·044	51·089
	0·3	3·221	15·343	17·157	37·081	48·265
	0·4	3·156	12·161	14·600	34·682	45·446
	0·5	3·057	8·948	13·714	30·551	41·733
II and full depth	0·1	3·311	16·886	35·532	38·552	54·119
	0·2	3·309	16·794	26·314	37·757	45·586
	0·3	3·308	16·764	17·356	36·544	40·443
	0·4	3·294	11·754	16·549	34·975	35·883
	0·5	3·293	8·390	16·473	31·679	33·341

TABLE 7

Frequency parameters $\sqrt{\rho t\omega^2 a^4/D}$ *for a square cantilevered plate (pretwist* = 60 *and thickness ratio* = 50) *for various crack types (full depth) and lengths in different modes*

Crack type	c/a	Mode 1	Mode 2	Mode 3	Mode 4	Mode 5
I and full depth	0·1	3·164	14·122	38·373	42·532	48·649
	0·2	3·142	13·799	26·930	42·154	48·063
	0·3	3·110	13·303	18·122	41·072	47·263
	0·4	3·056	12·138	13·258	38·260	46·068
	0·5	2·973	9·085	12·146	32·386	42·186
II and full depth	0·1	3·194	14·523	40·745	42·593	50·257
	0·2	3·187	14·428	28·744	42·086	48·108
	0·3	3·187	14·403	18·009	41·345	43·943
	0·4	3·167	11·907	14·207	39·618	40·162
	0·5	3·166	8·389	14·144	34·350	38·848

Specifically, the effects of cracks on rotors have been studied in references [5–8], and on vibrating beams in references [9–11]. A glance at the existing literature and reviews reveals that while extensive studies have been carried out on the dynamic effects of cracks in rotors, beams and columns, i.e., members which may be idealized as one-dimensional structural elements, work relating to the study of similar effects on plates and shells is relatively scarce.

The complexity of real structures prompts the requirement of the use of FEM over classical methods. In reference [12] point finite elements are used to model a cracked beam and in reference [13] finite elements are employed for the analysis of cracked axisymmetric

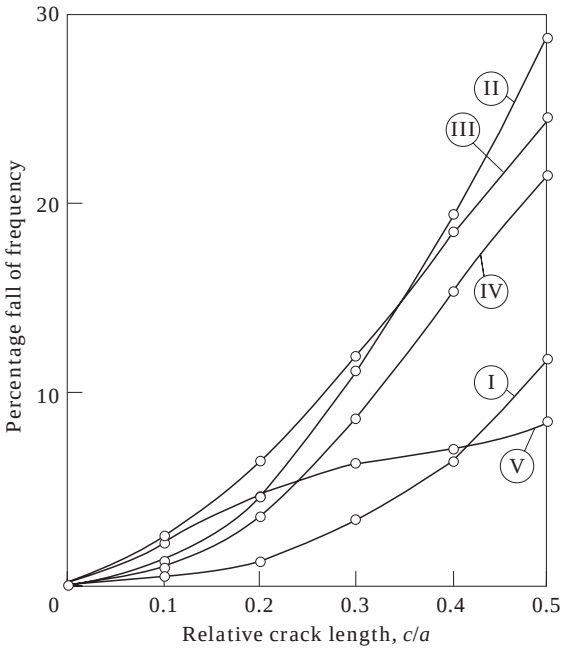

Figure 4. The drop in frequency for a blade with a type I crack (pretwist = 0). —, Brick and plate; mode numbers uncircled.

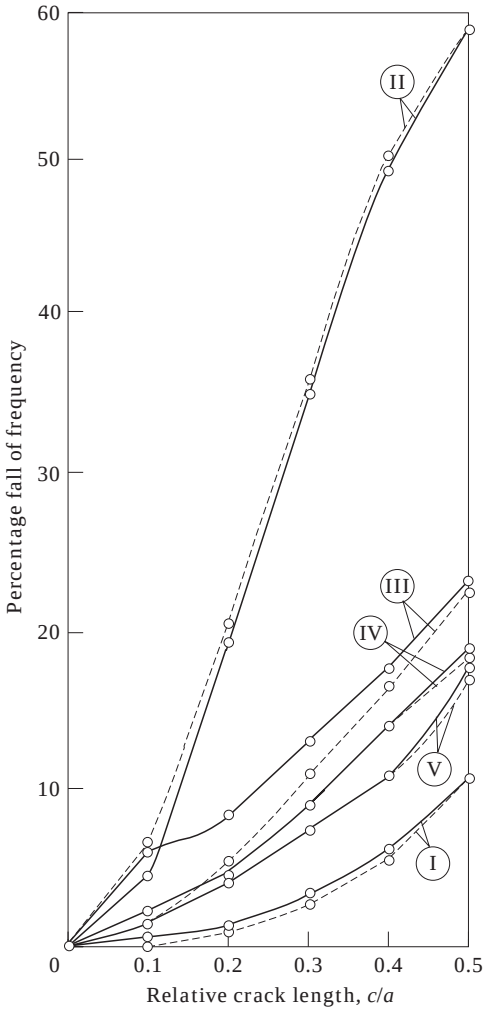

Figure 5. The drop in frequency for a blade with a type I crack (Pretwist = 15). --, Brick; —, plate; mode numbers uncircled.

structures subjected to torsional loading. Extensive work on the vibration and stability of a high aspect ratio cracked blade modelled as a beam has been carried out in references [14–16]. Furthermore, in reference [17] the dynamic stability of shaft–disc system with flaws has been also studied. In essence, the work devoted to the use of FEM to model damaged structures may be divided into two groups. The first group of researchers (references [18, 19]) use the method of separation of nodes to model the crack and the degree of mesh refinement depends on whether ordinary finite element or crack tip (quarter point) elements are employed. The focus of interest of such papers is largely conventional fracture mechanics. This approach has been used sparingly for the analysis of dynamic effects. The second group of researchers use finite elements with a crack to model the damaged structure. While in reference [20] this is used for the determination of the stress intensity factor, in reference [21] it is used to obtain the dynamic effects.

While the first approach requires handling of a relatively large problem, the second approach makes the element formulation considerably more complicated. An example of

such a relatively complex formulation as applied to the in-plane vibration of a cracked plate found in reference [22]. In the present work, we opt to follow the first approach. The necessity of such an attempt lies in obtaining results which may not only be of considerable practical interest but will also provide a benchmark, on the basis of which special elements may be developed in future for three-dimensional analysis of damaged bodies.

2.2. SOLUTION METHODS

2.2.1. *Element selection*

The eight-noded brick element with three degrees of freedom (dof) per node along with appropriate incompatible modes, as detailed in the next section, is employed.

The legitimate question that may be asked at the present point is as follows. Why has a 20-noded brick element not been used, even though it possesses the flexibility of using it as a crack tip element? In this regard, the authors feel that rapid mesh refinement is an

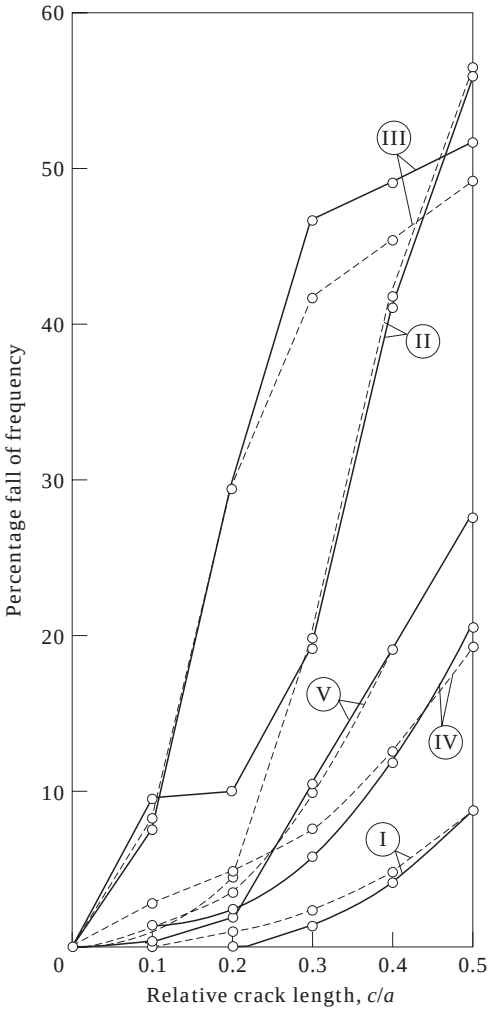

Figure 6. The drop in frequency for a blade with a type I crack (prewist = 30). Key as Figure 5.

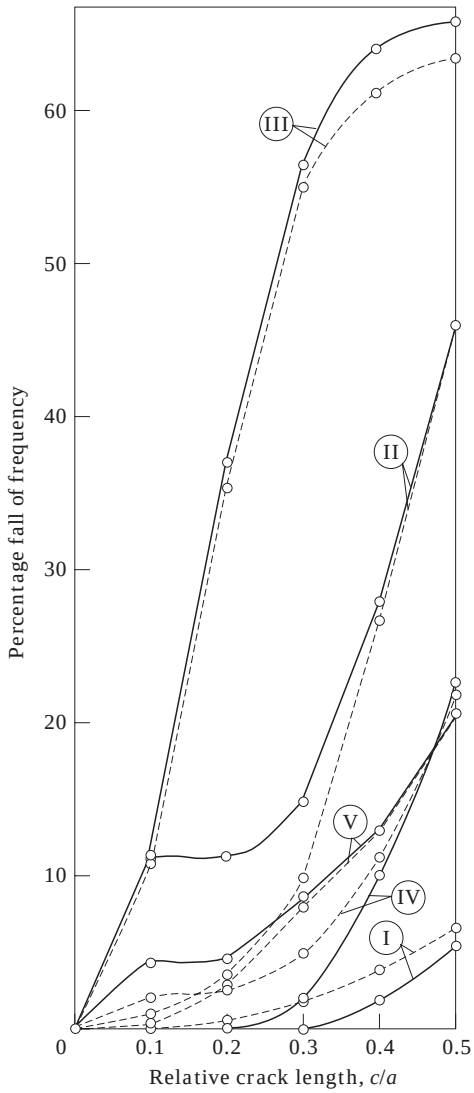

Figure 7. The drop in frequency for a blade with a type I crack (prewist = 45). Key as Figure 5.

established alternative for modelling crack tip singularities (stress singularity) and, in addition, since the natural frequency of a structure is largely dependent on the boundary conditions, one needs to use a large number of nodes (and so elements) at the crack face to model it closely. Therefore, the inherent advantage of using a crack tip element to reduce the size of the problem (by reducing the number of nodes/elements) does not appear to be of much benefit here.

2.2.2. *Shape function and incompatible modes*

The shape function of a basic linear solid element, as shown in Figure 1, is expressed as

$$N_i = \tfrac{1}{8}(1 \pm r)(1 \pm s)(1 \pm t), \qquad \text{for } i = 1, 8. \tag{1}$$

The displacement and co-ordinates of any point within the element are interpolated as

$$u = \sum_{i=1}^{8} N_i u_i \ldots \qquad \text{and} \qquad x = \sum_{i=1}^{8} N_i x_i \ldots . \tag{2}$$

These shape functions assure displacement continuity in the neighbouring elements.

The strain displacement matrix is expressed as

$$\underset{(6,24)}{[B]} = \underset{(6,9)}{[BA]}\,\underset{(9,24)}{[AB]}, \tag{3}$$

where the elements of $[BA]$ are elements of $[J]^{-1}$ ($[J]$ is Jacobian) properly arranged in order that $[BA]$ relates the strains to the derivatives of the displacement in the natural co-ordinate system, and $[AB]$ contains derivatives of u, v and w with respect to r, s and t, so that it relates derivatives of u, v and w in the natural co-ordinate system to u, v and w themselves.

The modulus matrix $[D]$ is as usual for a 3-D solid and the stiffness matrix $[K]$ is (24, 24).

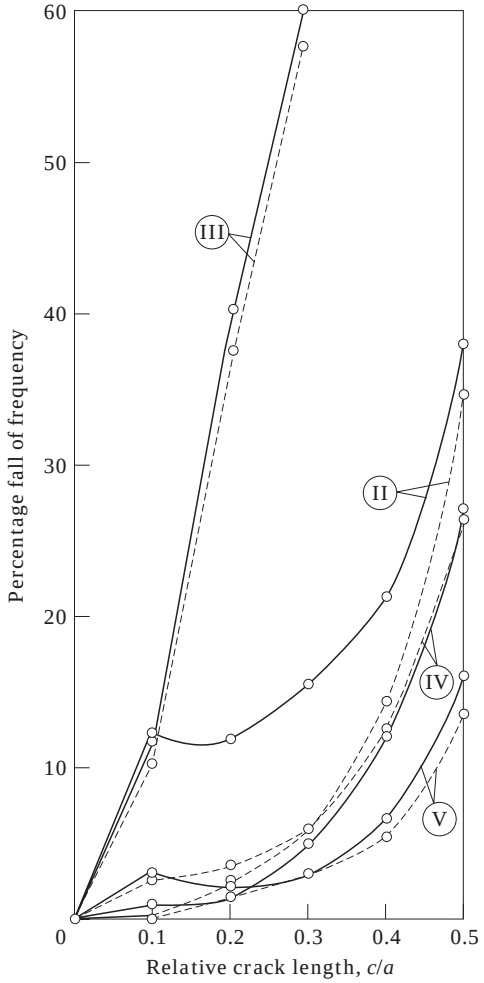

Figure 8. The drop in frequency for a blade with a type I crack (prewist = 60). Key as Figure 5.

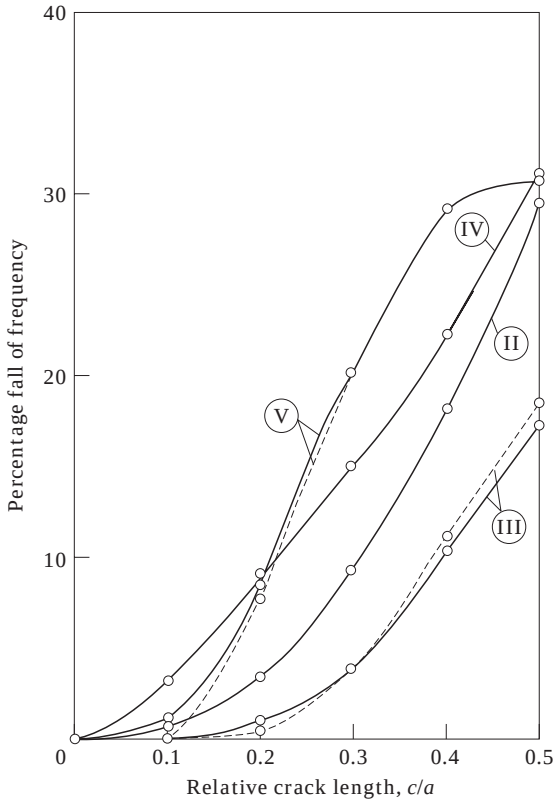

Figure 9. The drop in frequency for a blade with a type II crack (prewist = 0). Key as Figure 5.

Details of the element formulation are lucidly discussed in reference [23]. Since the shape functions assume a linear variation of the displacement along each of the axes r, s and t, the edges of the element remain straight after deformation and consequently the elements become too stiff for bending applications.

A fairly obvious solution to the problem suggested in reference [24] is the addition of three extra displacement modes attached to internal degrees of freedom, and so the displacement interpolation is modified to

$$u = \sum_{i=1}^{8} N_i u_i + \sum_{j=1}^{3} N_j' a_j \ldots \qquad \text{where } N_1' = 1 - r^2, \quad N_2' = 1 - s^2, \quad N_3' = 1 - t^2 \quad (4)$$

and the a_j are the nodeless degrees of freedom, whereas the co-ordinate interpolation remains the same as that in equation (2).

The strain–displacement matrix now becomes

$$[B'] = [BA'][AB'] = [BA'][[AB_{orig}] \quad [AB_{aug}]]$$
$$= [[BA_{orig}][AB_{orig}] \quad [BA_{aug}][AB_{aug}]] = [[B_{orig}] \quad [B_{aug}]], \quad (5)$$

in which the $[B_{orig}]$ is calculated as usual, whereas in the augmented $[B]$ matrix $[BA_{aug}]$ is the same as $[BA_{orig}]$, with the exception that the Jacobian matrix is calculated at the centroid of the element ($r = s = t = 0$) for an element of arbitrary shape, but for elements in the shape of a paralellopiped this restriction need not be imposed. This contrivance helps

the element to pass the patch test and has been discussed in detail in reference [25]. Furthermore, the matrix contains the additional contribution from the nodeless degree of freedom.

The stiffness matrix (along with contribution from incompatible modes) is (33, 33), and is expressed as

$$[K] = \begin{bmatrix} K_{RR} & K_{RC} \\ K_{CR} & K_{CC} \end{bmatrix}, \tag{6}$$

where $[K_{RR}]$ is (24, 24) and is identical to the stiffness matrix of the ordinary eight-noded brick element, whereas others are due to augmentation.

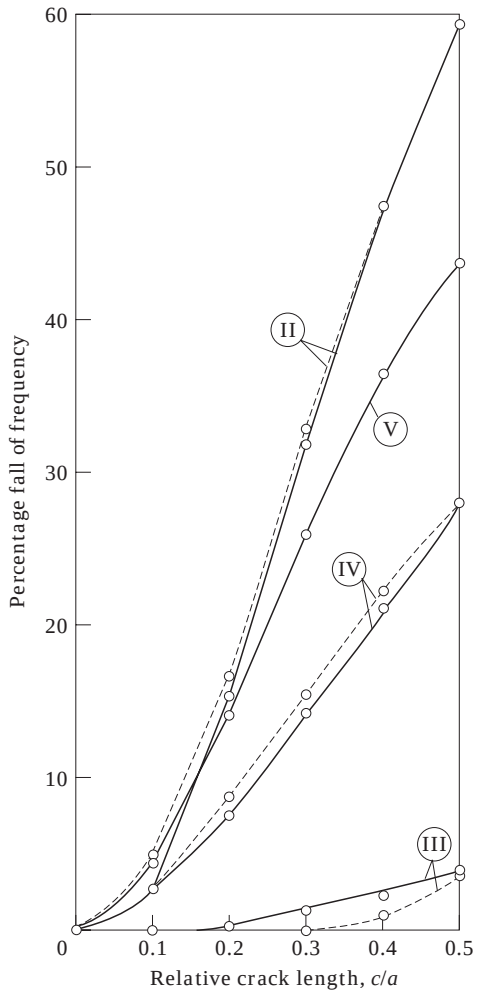

Figure 10. The drop in frequency for a blade with a type II crack (prewist = 15). Key as Figure 5.

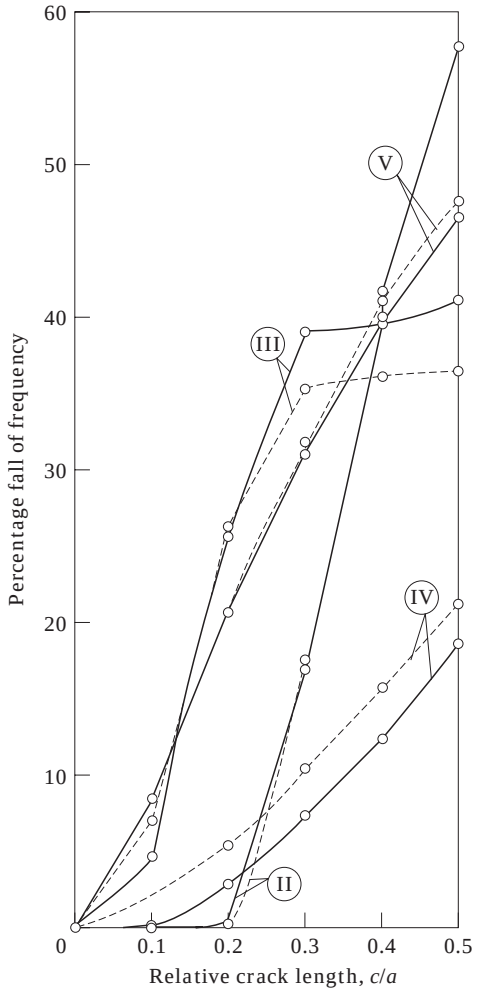

Figure 11. The drop in frequency for a blade with a type II crack (prewist = 30). Key as Figure 5.

In order to reduce the order of the stiffness matrix to (24, 24), the additional degrees of freedom are eliminated using static condensation: i.e.,

$$\text{condensed } [K] = [K_{RR}] - [K_{RC}][K_{CC}]^{-1}[K_{CR}]. \tag{7}$$

2.2.3. *The shell model*

A shell is a structure that can be derived from a flat plate by converting the middle plane to a curved surface, and so the pretwisted plate qualifies to be called a shell. Such a structure can be analyzed by finite elements by using either a flat plate element or a curved shell element, or a degenerated shell element or 3-D elements. Both the advantages and the disadvantages of using these approaches have been adequately dealt with in the finite element literature. As far as the modelling of a crack is concerned, the first three approaches can model only a full depth crack, while the last is capable of accommodating a partial depth crack, and therefore is the only choice for the present analysis.

3. VALIDATION

3.1. VALIDATION OF CODE

A finite element code using the element described in section 2.2.1 has been developed. The mass matrix used was lumped. After a skyline assembly of the element matrices, the lowest few eigenpairs were extracted by using the Lanczos method.

To ensure the flawlessness of the code developed, the non-dimensional frequency parameters obtained from the present code, tabulated in Table 1, were compared with those given in reference [26]. The table shows that the results are in close agreement.

3.2. VALIDATION OF THE DISCRETIZATION PATTERN

Two points of importance that one must consider during discretization of a given domain into finite elements are the E/V_e ratio (where E represents Young's modulus and V_e is the element volume) of a pair of neighbouring elements, and the aspect ratio of an element. According to reference [27], the E/V_e ratio for a pair of neighbouring elements should nowhere in the domain exceed 3, whereas no such rule of thumb for aspect ratio

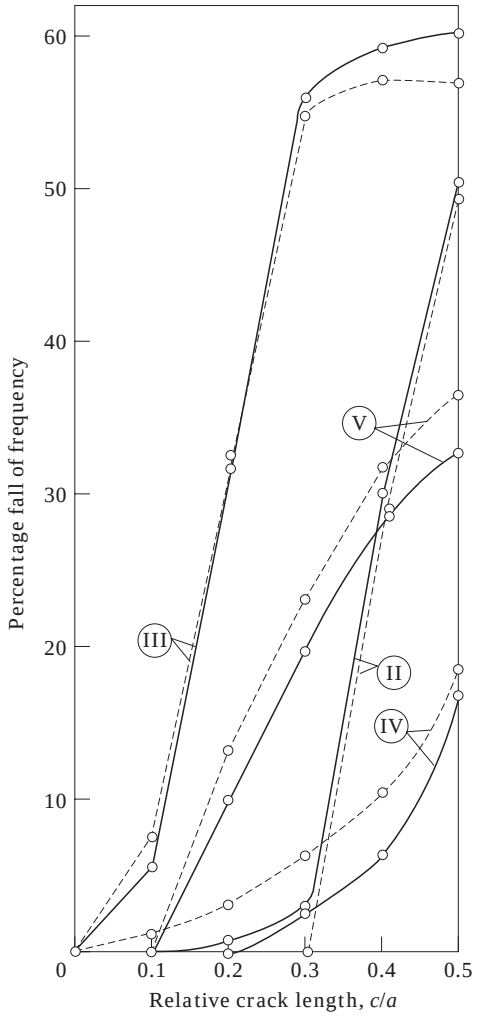

Figure 12. The drop in frequency for a blade with a type II crack (prewist = 45). Key as Figure 5.

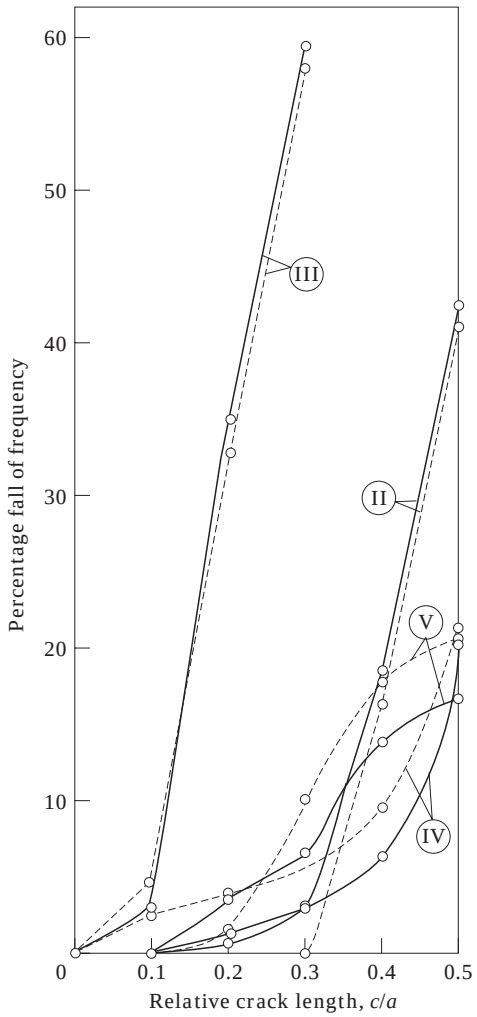

Figure 13. The drop in frequency for a blade with a type II crack (prewist = 60). Key as Figure 5.

of an element is within the knowledge of the authors. As such, a numerical experimentation was performed. Uncracked cantilevered plates were analyzed by using a 20×20 non-uniform mesh as shown in Figure 2, and the results are reported in Table 1. The maximum E/V_e ratio for a pair of neighbouring elements in this mesh is 2, and the aspect ratio of an element is 5. (The same non-uniform mesh was also used later to analyze the case of type I crack with a relative crack length of 0·5, and will be discussed in the next section.) The result obtained from such an analysis of the uncracked cantilevered plates was very close to that obtained using the 20×20 uniform mesh. This indicates that the discretization pattern (aspect ratio 5 and $E/V_e = 2$) does not inject any numerical error such that accuracy is effectively hampered.

4. CORE AND LABOUR

Although it has already been stated that the present technique requires handling of problems of a relatively large size, to give the readers a feel of the size and time that the

present element needs, the core and labour values while using the eight-noded 3-D brick element have been compared with those when a three-noded triangular plate element is used. Example data for a representative problem are given in Table 2. For other types of problems, the values may be still higher. It needs to be further stressed that while the latter may be run using a 386 with 8 MB RAM, the former requires a mainframe. Presently, an IBM RS 6000 mainframe system has been used.

5. COMPARISON OF RESULTS OF PLATE WITH FULL DEPTH CRACK

A cracked cantilever with a crack oriented parallel to the length or width has been considered. Two different configurations, as shown in Figure 3, are considered. For each orientation, crack lengths lying between 10% and 50% of the length or width, as applicable, and of depth ranging from 25% to 100% (full depth) of the thickness, have

TABLE 8

Frequency parameters $\sqrt{\rho t\omega^2 a^4/D}$ *for a square cantilevered untwisted plate for various crack types (partial depth) and lengths in different modes*

Crack type	c/a	Mode 1	Mode 2	Mode 3	Mode 4	Mode 5
I and	0·1	3·496	8·517	21·229	26·911	30·773
relative crack	0·2	3·496	8·523	21·213	26·855	30·770
depth = 0·25	0·3	3·496	8·524	21·198	26·822	30·764
	0·4	3·495	8·527	21·186	26·791	30·767
	0·5	3·495	8·526	21·172	26·750	30·770
I and	0·1	3·494	8·515	21·177	26·905	30·689
relative crack	0·2	3·491	8·518	21·091	26·838	30·596
depth = 0·50	0·3	3·488	8·517	21·010	26·789	30·533
	0·4	3·484	8·517	20·936	26·734	30·510
	0·5	3·481	8·515	20·864	26·663	30·507
I and	0·1	3·491	8·513	21·099	26·898	30·566
relative crack	0·2	3·479	8·514	20·804	26·809	30·218
depth = 0·75	0·3	3·464	8·510	20·461	26·717	29·957
	0·4	3·448	8·508	20·120	26·598	29·835
	0·5	3·431	8·503	19·790	26·456	29·807
II and	0·1	3·506	8·538	21·629	26·782	31·321
relative crack	0·2	3·507	8·540	21·531	26·744	31·207
depth = 0·25	0·3	3·507	8·541	21·497	26·714	31·177
	0·4	3·498	8·526	21·266	26·648	30·867
	0·5	3·498	8·526	21·229	26·625	30·813
II and	0·1	3·506	8·536	21·617	26·661	31·310
relative crack	0·2	3·507	8·538	21·507	26·465	31·182
depth = 0·50	0·3	3·507	8·537	21·465	26·289	31·142
	0·4	3·498	8·519	21·234	26·095	30·835
	0·5	3·498	8·517	21·197	25·969	30·769
II and	0·1	3·506	8·535	21·599	26·482	31·301
relative crack	0·2	3·507	8·535	21·439	25·839	31·164
depth = 0·75	0·3	3·507	8·533	21·338	25·164	31·115
	0·4	3·498	8·515	21·073	24·507	31·827
	0·5	3·498	8·511	21·004	24·005	30·736

TABLE 9

Frequency parameters $\sqrt{\rho t\omega^2 a^4/D}$ *for a square cantilevered plate (pretwist* = 15 *and thickness ratio* = 50*) for various crack types (partial depth) and length in different modes*

Crack type	c/a	Mode 1	Mode 2	Mode 3	Mode 4	Mode 5
I and	0·1	3·471	17·469	20·709	28·829	38·134
relative crack	0·2	3·471	17·481	20·694	28·778	38·129
depth = 0·25	0·3	3·471	17·480	20·679	28·743	38·125
	0·4	3·470	17·486	20·663	28·720	38·128
	0·5	3·470	17·481	20·649	28·678	38·129
I and	0·1	3·469	17·427	20·668	28·807	38·048
relative crack	0·2	3·467	17·427	20·585	28·751	37·971
depth = 0·50	0·3	3·463	17·426	20·493	28·715	37·930
	0·4	3·460	17·427	20·401	28·691	37·919
	0·5	3·456	17·408	20·315	28·642	37·917
I and	0·1	3·467	17·276	20·615	28·745	37·898
relative crack	0·2	3·456	17·145	20·365	28·663	37·582
depth = 0·75	0·3	3·442	17·117	20·030	28·624	37·387
	0·4	3·426	17·124	19·647	28·602	37·306
	0·5	3·410	17·082	19·265	28·550	37·286
II and	0·1	3·482	17·506	21·121	28·694	38·732
relative crack	0·2	3·483	17·503	21·022	28·660	38·604
depth = 0·25	0·3	3·483	17·503	20·989	28·636	38·547
	0·4	3·473	17·483	20·756	28·578	38·217
	0·5	3·473	17·483	20·718	28·561	38·144
II and	0·1	3·482	17·473	21·119	28·585	38·665
relative crack	0·2	3·483	17·461	21·017	28·414	38·523
depth = 0·50	0·3	3·483	17·460	20·985	28·264	38·437
	0·4	3·473	17·438	20·751	28·098	38·074
	0·5	3·473	17·434	20·713	27·992	37·983
II and	0·1	3·482	17·356	21·115	28·419	38·464
relative crack	0·2	3·483	17·251	21·006	27·849	38·279
depth = 0·75	0·3	3·483	17·231	20·969	27·270	38·147
	0·4	3·473	17·213	20·737	26·701	37·668
	0·5	3·473	17·204	20·699	26·238	37·473

been studied. It should be noted that root cracks or centre cracks have not been considered, because even for a full depth crack the potency of these cracks to reduce the natural frequency is low. Furthermore, centre cracks require unusually high degrees of freedom and probably would not be amenable to solution by in-core eigensolvers.

For the purpose of generating meshes, a simple but robust 3-D (solid) mesh generator using an array of hexahedra and a scheme following precisely the arguments of reference [28] has been used. The mesh has been refined towards the tip of the crack by specifying a progressively smaller element length while approaching the crack tip in either direction. As an illustrative example, the mesh pattern used for crack type I with relative crack length of 0·5 has been shown in Figure 2. Along the depth-wise direction, four elements have been taken, because this would not only permit analysis of cases with crack depths of 25%, 50%, 75% and 100% of the thickness, but also it would be preferable to use a multiple layer of eight-noded elements to simulate the bending behaviour of shell. However, it is felt that

a larger number of elements could have been taken, which would permit modelling of cracks of other depths as well. However, it should be noted that this would raise the problem size considerably, and the present discretization is probably good enough to indicate the trend clearly.

Numerical experimentation has been performed for both an untwisted plate and plates with pretwist angles of 15, 30, 45 and 60 degrees. The results are given in Tables 3–7. To obtain the co-ordinates of the nodes of the pretwisted plate from those of the untwisted plate, the condition of linear pretwist has been used.

It is preferable that one should compare the percentage fall in the natural frequency (or the non-dimensional natural frequency parameter) reported in this paper with those reported in reference [1], and not with the non-dimensional parameters themselves, as a fair amount of variation is expected (between results obtained by using triangular plate and brick elements) as reported in reference [26] (especially for higher pretwist angles and

TABLE 10

Frequency parameters $\sqrt{\rho t\omega^2 a^4/D}$ *for a square cantilevered plate (pretwist* $= 30$ *and thickness ratio* $= 50$*) for various crack types (partial depth) and length in different modes*

Crack type	c/a	Mode 1	Mode 2	Mode 3	Mode 4	Mode 5
I and	0·1	3·401	18·932	29·431	33·603	50·879
relative crack	0·2	3·400	18·917	29·430	33·557	50·830
depth = 0·25	0·3	3·400	18·904	29·421	33·512	50·811
	0·4	3·399	18·888	29·427	33·489	50·799
	0·5	3·398	18·874	29·412	33·445	50·795
I and	0·1	3·399	18·896	29·360	33·563	50·834
relative crack	0·2	3·396	18·820	29·339	33·514	50·751
depth = 0·50	0·3	3·393	18·739	29·329	33·462	50·721
	0·4	3·389	18·652	29·324	33·439	50·706
	0·5	3·385	18·567	29·289	33·395	50·702
I and	0·1	3·397	18·837	29·095	33·431	50·746
relative crack	0·2	3·387	18·587	28·899	33·358	50·538
depth = 0·75	0·3	3·375	18·285	28·876	33·292	50·449
	0·4	3·360	17·964	28·839	33·256	50·419
	0·5	3·344	17·636	28·723	33·208	50·413
II and	0·1	3·413	19·305	29·457	33·506	51·644
relative crack	0·2	3·412	19·211	29·449	33·469	51·446
depth = 0·25	0·3	3·412	19·184	29·449	33·453	51·312
	0·4	3·402	18·972	29·417	33·381	50·845
	0·5	3·401	18·939	29·416	33·372	50·765
II and	0·1	3·413	19·305	29·392	33·434	51·489
relative crack	0·2	3·413	19·211	29·370	33·311	51·272
depth = 0·50	0·3	3·412	19·184	29·369	33·218	51·076
	0·4	3·402	18·969	29·335	33·080	50·552
	0·5	3·401	18·932	29·329	33·014	50·450
II and	0·1	3·413	19·305	29·146	33·329	50·974
relative crack	0·2	3·413	19·211	28·957	32·979	50·680
depth = 0·75	0·3	3·412	19·183	28·933	32·637	50·367
	0·4	3·402	18·963	28·907	32·251	49·601
	0·5	3·401	18·915	28·899	31·949	49·328

TABLE 11

Frequency parameters $\sqrt{\rho t\omega^2 a^4/D}$ *for a square cantilevered plate (pretwist* $= 45$ *and thickness ratio* $= 50$*) for various crack types (partial depth) and lengths in different modes*

Crack type	c/a	Mode 1	Mode 2	Mode 3	Mode 4	Mode 5
I and	0·1	3·295	16·562	38·141	38·996	52·554
relative crack	0·2	3·293	16·546	38·111	38·914	52·535
depth = 0·25	0·3	3·293	16·535	38·106	38·830	52·542
	0·4	3·291	16·519	38·212	38·688	52·532
	0·5	3·291	16·507	38·188	38·644	52·537
I and	0·1	3·294	16·534	38·112	38·893	52·552
relative crack	0·2	3·290	16·471	38·066	38·809	52·531
depth = 0·50	0·3	3·287	16·405	38·056	38·714	52·538
	0·4	3·283	16·327	38·099	38·617	52·527
	0·5	3·279	16·249	38·054	38·579	52·532
I and	0·1	3·292	16·487	37·927	38·595	52·547
relative crack	0·2	3·283	16·291	37·684	38·508	52·521
depth = 0·75	0·3	3·273	16·053	37·640	38·410	52·526
	0·4	3·259	15·778	37·460	38·457	52·515
	0·5	3·243	15·485	37·322	38·424	52·519
II and	0·1	3·311	16·885	38·237	38·794	54·349
relative crack	0·2	3·308	16·794	38·223	38·739	53·694
depth = 0·25	0·3	3·308	16·774	38·225	38·721	53·431
	0·4	3·294	16·587	38·190	38·615	52·469
	0·5	3·293	16·562	38·190	38·614	52·512
II and	0·1	3·311	16·885	38·160	38·760	54·342
relative crack	0·2	3·308	16·794	38·130	38·666	53·670
depth = 0·50	0·3	3·308	16·773	38·131	38·612	53·378
	0·4	3·294	16·582	38·094	38·475	52·384
	0·5	3·293	16·551	38·094	38·443	52·413
II and	0·1	3·311	16·885	37·856	38·731	54·330
relative crack	0·2	3·308	16·794	37·618	38·590	53·616
depth = 0·75	0·3	3·308	16·770	37·582	38·447	53·252
	0·4	3·294	16·571	37·537	38·204	52·159
	0·5	3·293	16·527	37·533	38·053	52·118

higher modes). As such, the percentage drop in frequency has been plotted with relative crack length in Figures 4–13.

It is found from the graphs that the percentage falls of natural frequency by the two methods are in excellent coherence for untwisted plates and in fair agreement for pretwist up to 30 degrees. However, for high values of pretwist (45 and 60 degrees), differences do exist.

6. RESULTS OF PLATE WITH PARTIAL DEPTH CRACK AND INTERPRETATION

Analysis as described in the previous section has been performed and results for various crack depths and pretwist angles have been tabulated in Tables 8–12. On the basis of these tables, Table 13 has been prepared for an easy and effective interpretation of results. In Table 13 is shown the percentage drop in the natural frequency for full depth cracks

(analyzed by solid and plate elements), as well as the same value for the largest possible partial depth crack (relative crack length = 0·5 and relative crack depth = 0·75). This clearly brings out the following points:

(1) As mentioned earlier, the coherence between the values obtained by using plate element and brick element is quite good.

(2) For a partial depth type II crack, for all values of the pretwist angle, the maximum drop in the natural frequency is observed in mode 4, and this value decreases as the pretwist angle increases. For a partial depth type I crack, the maximum drop in the natural frequency is found in mode 3 for pretwist angles of 10 and 15 degrees, whereas for higher values it appears in mode 2.

(3) The maximum values of the percentage drop in the natural frequency for a partial

TABLE 12

Frequency parameters $\sqrt{\rho t\omega^2 a^4/D}$ *for a square cantilevered plate (pretwist* = 60 *and thickness ratio* = 50*) for various crack types (partial depth) and lengths in different modes*

Crack type	c/a	Mode 1	Mode 2	Mode 3	Mode 4	Mode 5
I and	0·1	3·170	14·232	42·267	43·764	48·916
relative crack	0·2	3·167	14·214	42·219	43·608	48·871
depth = 0·25	0·3	3·167	14·205	42·194	43·515	48·864
	0·4	3·164	14·188	42·259	43·384	48·843
	0·5	3·164	14·178	42·228	43·355	48·843
I and	0·1	3·169	14·212	42·254	43·659	48·899
relative crack	0·2	3·164	14·160	42·204	43·491	48·850
depth = 0·50	0·3	3·162	14·107	42·161	43·398	48·844
	0·4	3·157	14·037	42·179	43·293	48·824
	0·5	3·154	13·969	42·137	43·263	48·824
I and	0·1	3·168	14·177	42·180	43·284	48·853
relative crack	0·2	3·159	14·027	42·108	42·983	48·781
depth = 0·75	0·3	3·151	13·842	41·999	42·917	48·776
	0·4	3·137	13·610	41·770	42·966	48·757
	0·5	3·122	13·354	41·638	42·943	48·747
II and	0·1	3·194	14·523	42·694	43·399	50·321
relative crack	0·2	3·187	14·430	42·538	43·373	49·746
depth = 0·25	0·3	3·187	14·414	42·476	43·380	49·549
	0·4	3·167	14·243	42·215	48·350	48·774
	0·5	3·167	14·223	42·230	43·358	48·816
II and	0·1	3·194	14·523	42·676	43·345	50·311
relative crack	0·2	3·187	14·429	42·508	43·314	49·715
depth = 0·50	0·3	3·187	14·412	42·441	43·317	49·485
	0·4	3·167	14·238	42·180	43·284	48·672
	0·5	3·166	14·213	42·190	43·290	48·694
II and	0·1	3·194	14·523	42·628	43·154	50·295
relative crack	0·2	3·187	14·429	42·394	43·063	49·648
depth = 0·75	0·3	3·187	14·409	42·310	43·059	49·333
	0·4	3·167	14·227	42·060	43·004	48·401
	0·5	3·166	14·190	42·053	42·996	48·342

TABLE 13

The percentage drop in natural frequency for a full depth crack and the largest partial depth crack (relative crack length = 0·5 and thickness ratio = 0·75) for crack types I and II

Pretwist	Crack type	Case	Mode 1	Mode 2	Mode 3	Mode 4	Mode 5
0	I	1	1	N	7	2	3
		2	12	29	25	21	8
		3	12	29	25	22	9
	II	1	N	N	1	11	N
		2	N	29	18	30	30
		3	N	29	17	31	30
15	I	1	1	2	7	1	3
		2	11	59	22	18	17
		3	11	59	23	19	18
	II	1	N	2	N	9	2
		2	N	59	4	27	44
		3	N	59	4	27	43
30	I	1	1	7	3	2	2
		2	8	56	48	19	27
		3	8	55	51	20	27
	II	1	N	N	2	5	4
		2	N	57	36	21	47
		3	N	58	41	18	46
45	I	1	1	6	3	2	N
		2	7	46	64	22	21
		3	6	46	66	23	21
	II	1	N	N	2	3	1
		2	N	49	57	19	37
		3	N	50	61	17	33
60	I	1	N	6	2	2	N
		2	5	36	72	26	14
		3	4	38	73	27	16
	II	1	N	N	1	2	1
		2	N	41	67	21	20
		3	N	42	70	20	17

Case 1 represents a partial depth crack analyzed by 3-D FE analysis.
Case 2 represents a full depth crack analyzed by 3-D FE analysis.
Case 3 represents a full depth crack analyzed by using plate elements [1].
N represents almost no change (<1%).

depth and a full depth crack of a definite type and a specified pretwist need not necessarily occur for the same mode.

(4) The values for the percentage drop for a full depth crack in a definite mode (for a definite type of crack of given relative width and pretwist angle) are much higher than those of the (largest) partial depth crack.

(5) From Tables 3–12, it can clearly be seen that, for a full depth crack, the crack width is an important parameter controlling the natural frequency, whereas for a partial depth crack in most of the cases, the natural frequency becomes insensitive to crack length.

It has been pointed out in reference [1] that the physical reason why cracks lower the natural frequency is the local flexibility in the vicinity of the crack which, in turn, reduces the overall stiffness of the structure. In the light of this statement, the inferences in points

(4) and (5) above become obvious. It should be mentioned that although example mode shapes are shown in reference [1], they are not illustrated here, because not only are the changes for the partial depth cracks marginal, but also storing modal vectors of such large size and consequent post-processing by using graphics routines is difficult.

7. CONCLUSIONS

In the present work, a cracked three-dimensional object has been modelled by using eight-noded brick element (with incompatible modes) and the method of rapid mesh refinement. Results for an untwisted cracked blade (with a full depth crack) have been compared with an earlier investigation and excellent coherence has been obtained. Results for a twisted cracked blade (full depth crack) have also been compared with the same reference and found to be fairly satisfactory. The case of partial depth crack on blades has been studied for both untwisted and pretwisted blades. As observed earlier, it appears that the natural frequency is not a very attractive parameter for full depth crack diagnosis and for partial depth cracks, the effect being almost nil in many of the cases. However, experimental verification is suggested before drawing a final conclusion. Last but not least, it will not be prudent to extrapolate the conclusion for rotating structures where the stiffness (geometric) becomes dependent on the stress field, and, since the crack modifies the stress field in the vicinity of its tip, considerable changes may be produced in the dynamic effect.

REFERENCES

1. S. Neogy and V. Ramamush *Mechanics of Structures & Machines* (communicated). Effects of crack on the natural frequency of twisted plates—a finite element solution.
2. J. Wauer 1990 *Applied Mechanics Review* **43**(1), 13–17. On the dynamics of cracked rotors: a literature survey.
3. R. Gasch 1993 *Journal of Sound and Vibration* **160**, 313–332. A survey of the dynamic behaviour of a simple rotating shaft with a transverse crack.
4. A. D. Dimarogonas 1995 *Journal of Sound and Vibration* **188**, 297. Vibration of cracked structures database (letter to the editor).
5. A. D. Dimarogonas and C. A. Papadopoulos 1983 *Journal of Sound and Vibration* **91**, 583–593. Vibration of cracked shafts in bending.
6. C. A. Papadopoulos and A. D. Dimarogonas 1988 *Transactions of the American Society of Mechanical Engineers*, *Journal of Vibration*, *Acoustics*, *Stress and Reliability* **110**, 356–359. Stability of cracked rotors in coupled vibration mode.
7. C. A. Papadopoulus and A. D. Dimarogonas 1987 *Journal of Sound and Vibration* **117**, 81–93. Coupled longitudinal and bending vibration of a rotating shaft with an open crack.
8. S. C. Huang, Y. M. Huang and S. M. Shieh 1993 *Journal of Sound and Vibration* **162**, 387–401. Vibration and stability of a rotating shaft containing a transverse crack.
9. C. A. Papadopoulos and A. D. Dimarogonas 1992 *Transactions of the American Society of Mechanical Engineering*, *Journal of Vibration*, *Acoustics*, *Stress and Reliability* **114**, 461–467. Coupled vibration of cracked shafts.
10. C. A. Papadopoulos and A. D. Dimarogonas 1988 *Transactions of the American Society of Mechanical Engineering*, *Journal of Vibration*, *Acoustics*, *Stress and Reliability* **110**, 1–8. Coupled longitudinal and bending vibrations of a cracked shaft.
11. G. L. Qian, S. N. Gu and J. S. Jiang 1990 *Journal of Sound and Vibration* **138**, 233–243. The dynamic behaviour and crack detection of a beam with a crack.
12. W. M. Ostachowicz and M. Krawczuk 1990 *Computers and Structures* **36**(2), 245–250. Vibration analysis of a cracked beam.
13. W. H. Chen and H. L. Wang 1996 *Engineering Fracture Mechanics* **23**(4), 705–717. Finite element analysis of axi-symmetric cracked solid subjected to torsional loading.
14. L. W. Chen and J. L. Chen 1990 *Computers and Structures* **35**(6), 653–660. Non-conservative stability of cracked thick rotating blade.

15. L. W. Chen and C. H. Jeng 1993 *Computers and Structures* **43,** 133–140. Vibrational analysis of cracked pretwisted blades.
16. L. W. Chen and C. L. Chen 1988 *Computers and Structures* **28,** 67–74. Vibration and stability of cracked thick rotating blades.
17. D. M. Ku and L. W. Chen 1992 *Computers and Structures* **43**, 306–311. Dynamic stability of shaft–disc system with flaws.
18. R. S. Barsoum 1975 *International Journal for Numerical Methods in Engineering* **10**, 25–37. On the use of isoparametric finite elements in linear fracture mechanics.
19. R. D. Henshell and K. G. Shaw 1975 *International Journal for Numerical Methods in Engineering* **9**, 495–507. Crack tip finite elements are unnecessary.
20. E. Byskov 1970 *International Journal of Fracture Mechanics* **6**(2), 159–167. The calculation of stress intensity factor using finite element method with cracked element.
21. G. Gounaris and A. Dimarogonas 1988 *Computers and Structures* **28**(3), 309–313. Finite element of a cracked prismatic beam for structural analysis.
22. M. Krawczuk 1993 *Computers and Structures* **46**(3), 487–493. A rectangular plate finite element with an open crack.
23. V. Ramamurti 1996 *Computer Aided Mechanical Design and Analysis*. Tata McGraw Hill; third edition.
24. E. L. Wilson, R. L. Taylor, W. P. Doherty and T. Ghabussi 1973 *Numerical and Computer Methods in Structural Mechanics* (eds S. T. Fenves *et al*.) 43–57. Incompatible displacement models.
25. R. L. Taylor, P. J. Beresford and E. L. Wilson 1976 *International Journal for Numerical Methods in Engineering* **10**, 1211–1220. A non-conforming element for stress analysis.
26. *NASA Reference Publication no*. 1150, 1985. Joint research effort on vibrations of twisted plates.
27. R. D. Cook, D. S. Malkhus and M. E. Plesha 1989 *Concepts and Applications of Finite Element Analysis*. John Wiley; third edition.
28. O. C. Zienkiewicz and D. V. Philips 1971 *International Journal for Numerical Methods in Engineering* **3**, 519–528. An automatic mesh generation scheme for plane and curved surfaces by isoparametric co-ordinates.